[56] J. Peeters and C. Vinckier, 15th Symp. (Int.) on Combustion, The Combustion Institute, Pittsburgh 1974, p. 969.
[57] S. J. Arnold, G. H. Kimbell, and D. R. Snelling, Can. J. Chem. *53*, 2419 (1975).
[58] A. Fontijn and S. E. Johnson, J. Chem. Phys. *59*, 6193 (1973).
[59] A. Fontijn, private communication Nov. 1980.
[60] F. F. Martinotti, M. J. Welch, and A. P. Wolf, J. Chem. Soc., Chem. Commun. 115 (1968).
[61] R. Bleekrode and W. C. Nieuwpoort, J. Chem. Phys. *43*, 3680 (1965).
[62] K. H. Becker and D. Kley, Chem. Phys. Lett. *4*, 62 (1969).
[63] J. R. McDonald, A. P. Baronavski, and V. M. Donnelly, Chem. Phys. *33*, 161 (1978).

(Eingegangen am 22. Februar 1982) E 5145

VUV Flash Photolysis Study of the Reaction of HO with HO_2 at 1 atm and 298 K

M. Braun, A. Hofzumahaus, and F. Stuhl

Physikalische Chemie I, Ruhr-Universität, D-4630 Bochum, W.-Germany

Freie Radikale / Gase / Photochemie / Reaktionskinetik

Equal concentrations of HO and H were generated by flash photolysing small amounts of H_2O diluted in N_2 at a pressure of about one atmosphere. Using sensitive detection by resonance absorption, the HO radicals were monitored in the presence and in the absence of O_2. In the presence of O_2, the radicals were found to disappear significantly faster than in the absence of O_2. This enhanced decay is attributed to the fast reaction of HO with HO_2. Using simple kinetic arguments and computer modeling, the rate constant, k_1, for the title reaction is estimated to be $1.1 \cdot 10^{-10}$ cm^3 s^{-1} (+25%; −35%).

Introduction

Previously, the kinetics of the reaction of HO radicals with CO has been investigated in our laboratory at total pressures of up to 1000 mbar N_2 [1]. At that time the rate constant of this reaction was found to depend on total pressure when small amounts of O_2 were added to the reaction system. Since then we have improved the experimental arrangement and are now able to generate larger concentrations of HO the decay of which can be followed for longer times with higher precision. With this more sensitive method the HO radicals were observed to decay non-exponentially in the presence of excess CO and O_2. Subsequent computer modeling indicated that reactions of HO_2 can play an important role in this system. We have therefore begun a reinvestigation of the flash photochemistry of H_2O in the presence and in the absence of O_2. In the presence of O_2, the reaction of HO with HO_2 was found to be dominant. This photolysis system hence presents an opportunity for the study of this important radical radical reaction.

The reaction of HO with HO_2 is of importance to the understanding of combustion processes and of atmospheric chemistry. A significant feature of the reaction

$$HO + HO_2 \rightarrow H_2O + O_2 \qquad (1)$$

is the termination of two reactive radicals in HO_x(HO + HO_2) chain reactions [2].

The kinetics of reaction (1) has been previously investigated by a number of research groups [3–18]. While the values measured for the rate constant of this reaction range from $2 \cdot 10^{-11}$ to $2 \cdot 10^{-10}$ cm^3 s^{-1}, no review or evaluation [19–25] has recommended a value greater than $4 \cdot 10^{-11}$ cm^3 s^{-1}. It is interesting to note that the smaller values of k_1 have been obtained in flow systems at low total pressures while the larger values have been determined in irradiation systems at pressures of about one atmosphere.

In the present investigation, equal amounts of H and HO were generated by photolysing H_2O in N_2 at a pressure of about one atmosphere. The absolute concentration of HO was determined by time resolved absorption spectroscopy. Decays of HO were monitored in the absence and in the presence of O_2. In the absence of O_2, the major removal steps for HO are found to be the termolecular reactions of HO with H and HO. In the presence of O_2, H atoms are rapidly converted to HO_2 which in turn reacts dominantly with HO. It will be shown that the fast removal of HO in the presence of O_2 supports a fast rate constant, k_1, for reaction (1).

Experimental

Vacuum UV flash photolysis of H_2O was used to generate H and HO in the presence of N_2 at a pressure of about 1000 mbar and at a temperature of (298 ± 2 K). The apparatus has been described previously in detail [1]. For the present experiments, new LiF windows (Harshaw) with higher vuv transmission were used to generate initial concentrations of HO ranging from $1 \cdot 10^{12}$ to $7.3 \cdot 10^{12}$ cm^{-3}.

Since some of the relevant reactions in the present system proceed according to second order the accurate determination of the absolute radical concentration is very important. In these experiments, HO radicals were detected using absorption of light from an HO resonance lamp [1, 26]. The absorption light path was 11.2 m. The wavelength of detection was centered at 308.2 nm (HO($A^2\Sigma^+ \leftarrow X^2\Pi$); $Q_1(3)$ line) using a spectral resolution of about 0.2 nm.

Absolute concentrations of HO were calculated according to the relationship given by Golden et al [26]. Values of oscillator strengths of single rotational lines, $f_{J''J'}$, were estimated using $f_{00} = 7.05 \cdot 10^{-4}$ [26] and line strengths, $S_{J''J'}$, given by Goldman and Gillis [27]. For low rotational quanta, the corresponding temperature of the HO emission spectrum was measured to be 600 K. The rotational partition function was calculated to be Q_{rot} (298 K) = 40.5. With this data, the following

Note Added in Proof:

Another study [37] dealing with Reaction (1) at pressures of He and Ar ranging from 75 to 730 Torr has appeared since the submission of the present paper. The value for the rate constant at 1 atm pressure (k_1 = $1.2 \pm 0.4) \cdot 10^{-10}$ cm^3 s^{-1}) determined in this study is in very good agreement with that of the present investigation.

relationship for the incident and for the transmitted HO light intensities, I_0 and I, is obtained:

$$\ln(I_0/I) = 1.97 \cdot 10^{-13}(\pm 10\%) \cdot F \cdot [\mathrm{HO}]\,\mathrm{cm}^3 . \quad (\mathrm{I})$$

The dimensionless factor F in this equation takes into account pressure broadening of the absorbing lines. The estimated error limits do not include the uncertainty of the values of $f_{J''J'}$ but take into consideration the uncertainty of the measured rotational temperature of the HO emission and the finite spectral resolution of the detection system. Because of the finite resolution not only light of the $Q_1(3)$ line was received by the detector but also light of the $Q_{21}(3)$, $P_1(1)$, $Q_1(2)$, $Q_{21}(2)$, $Q_1(4)$, and $Q_{21}(4)$ lines. Therefore, the absorption of each of these lines was weighed accordingly.

The factor F is unity at low pressures. Values of this factor were determined experimentally for different pressures of N_2 ranging from 27 to 980 mbar. These values and those reported in the literature [1, 28–30] are displayed in Fig. 1. To obtain the present data for F, the initial absorption at constant pressure of N_2 was measured as a function of pressure of H_2O. It was observed in these runs that the absorption increases linearly with pressure of H_2O up to an absorption of 30%. From Fig. 1, for N_2 at a pressure of 980 mbar, a value of $F = 0.5$ was chosen which was estimated to be accurate within ±10%.

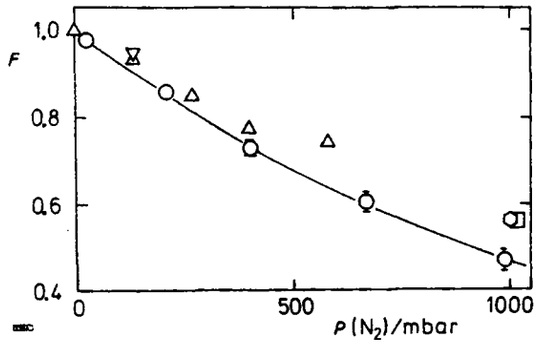

Fig. 1
The dependence of the factor F in Eq. (I) on pressure of added N_2 (○). F corrects the absorbance of HO with regard to collision broadening. The absorption lines are mentioned in the text. The error limits represent three times the standard deviation. The results of previous work are included: △, Ref. 30; □, Ref. 29; ◊, Ref. 1; ▽, Ref. 28

The flash lamp consisted of twelve electrodes equally spaced in front of the photolysis cell. The distance between the electrodes and the LiF windows was 5 cm. The lamp was purged with pure N_2 or, in most runs, with a mixture of N_2 and O_2 (up to 21 mbar O_2). This admixture of O_2 was used to prevent the photolysis of small amounts of O_2 which were added to the photolysis system in a number of experiments. Since second order reactions were to be studied the distribution of the radical concentration in the reactor has to be considered. Therefore, the variation of the intensity of several single flash electrodes was monitored using a photodiode. The shot to shot and electrode to electrode fluctuations of the intensity were found to stay well within ±30%.

The reactants (N_2, H_2O, and O_2) were introduced into the photolysis cell under slow flow conditions (≈20 $\mathrm{cm}^3\,\mathrm{s}^{-1}$). The previous flow system used to mix the reactants was simplified and modified to consist of metal and glass only. Connections were made of teflon or viton seals. The leak rate of the flow system was much smaller than that of the photolysis cell ($< 1 \cdot 10^{-5}$ mbar s^{-1}). The gases used had the following stated (Messer-Griesheim) minimum purities: N_2, 99.999%; O_2, 99.995%. Nitrogen was further purified by Oxisorb (Messer-Griesheim) which is stated by the manufacturer to remove O_2 to smaller than 0.1 ppm in the sample. Oxygen was premixed with N_2 before it was introduced into the flow; the H_2O sample was distilled three times and thoroughly degassed.

Results

Mixtures of H_2O and N_2 were flash photolysed at total pressures ranging from 970 to 1000 mbar. Partial pressures of H_2O ranged from 0.245 to 2.72 mbar. Most of the experiments were performed at H_2O pressures around 0.5 mbar. Initial concentrations of HO (and thus H) ranging from $1 \cdot 10^{12}$ to $7.3 \cdot 10^{12}$ cm^{-3} were generated in this photolysis system. In a number of experiments, small amounts of O_2 (0.037 to 0.47 mbar) were added in order to convert the H atoms rapidly to HO_2 radicals. To prevent the photolytical formation of O atoms, the flash lamp was flushed with mixtures of N_2 and O_2 at partial pressures of O_2 ranging from 5 to 21 mbar.

Typical decays of HO radicals in the presence and in the absence of small amounts of O_2 are shown in Fig. 2. These decay curves were obtained by averaging 128 single decays of HO in the memory of the multichannel analyser (Tracor NS 570A). Clearly, the addition of O_2 shortens the lifetime of HO. As will be discussed later, reactions which are second order in the concentration of HO are expected to be dominant at the beginning of the reaction. Therefore, in Fig. 2, the reciprocal of the absolute concentration of HO is plotted vs. reaction time. The dashed lines in this figure represent the slopes of the experimental curves at short reaction times and are thus taken to be representative for second order decays of HO during the initial stage of the reaction. As will be shown later, one way to estimate the value of k_1 is to use these initial slopes.

Another method will use a scheme of 16 reactions to simulate the decays of HO using a computer. The result of this computer modeling is displayed in Fig. 2 by full lines. In the present work, the HO decay curves were evaluated according to both these procedures.

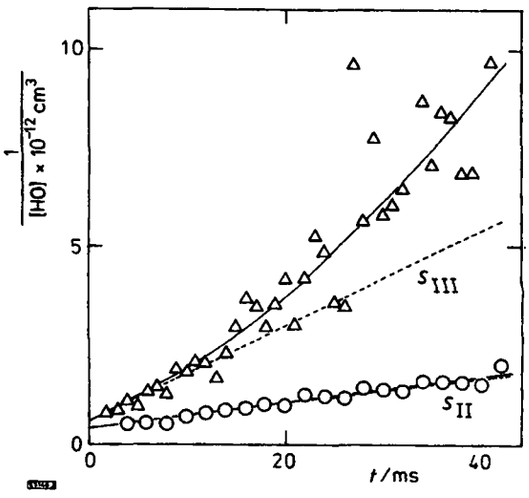

Fig. 2
Reciprocal of the absolute concentration of HO plotted vs. reaction time. The initial slopes of the curves, S_{II} and S_{III}, are represented by dashed lines. Computer simulations (see discussion) are displayed by full lines. For the lower curve the full line coincides with the dashed line. ○, without O_2 and △, with O_2 present. The respective runs are marked in Table 1 and 2 by asteriks

It is evident from Fig. 2 that the single data points scatter considerably in these flash photolysis experiments using time resolved absorption spectroscopy of low concentrations of HO at one atmosphere of N_2. Therefore, 85 decay curves of HO were recorded in order to improve the statistical significance of the results. These runs including their experimental conditions are listed in Tables 1 and 2. The last columns of Table 1 and Table 2 display the initial slopes resulting from plots like those given in Fig. 2. In Table 2, the runs are arranged in the order of increasing pressure of O_2 in the reaction system. For similar pressures of O_2, the runs are listed according to H_2O pressures. It can be easily seen that, while the slopes in the absence of O_2 range from $1.9 \cdot 10^{-11}$ to $5.0 \cdot 10^{-11}$ $\mathrm{cm}^3\,\mathrm{s}^{-1}$ (Table 1), the slopes in the presence of O_2 are much larger ranging from $9.5 \cdot 10^{-11}$ to $1.8 \cdot 10^{-10}$ $\mathrm{cm}^3\,\mathrm{s}^{-1}$ (Table 2). No trend is evident for the concentrations of H_2O and HO used in the

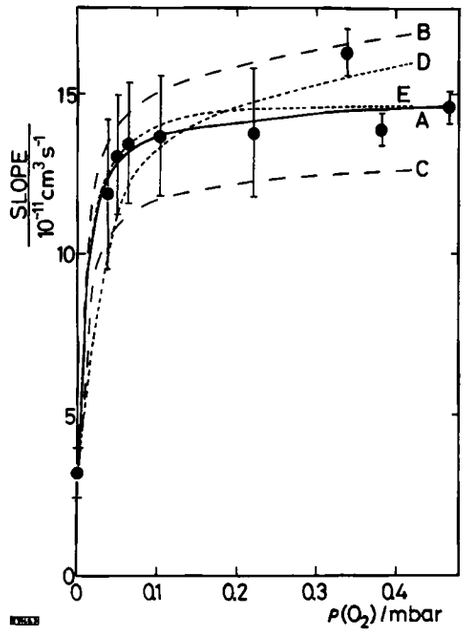

Fig. 3
The dependence of the initial overall second order rate constants for the removal of HO radicals on the partial pressure of O_2. The rate constants were obtained from the initial slopes of plots like those in Fig. 2. ●, experimental data, the error bars represent the standard deviation; A, calculated curve using the data of Table 3 and $[HO]_0 = 2.55 \cdot 10^{12}$ cm^{-3}; B, same as A, but $k_1 = 1.25 \cdot 10^{-10}$ cm^3 s^{-1}; C, same as A, but $k_1 = 8.5 \cdot 10^{-11}$ cm^3 s^{-1}; D, same as A, but $[HO]_0 = 6 \cdot 10^{12}$ cm^{-3}; E, same as A, but $[HO]_0 = 1.1 \cdot 10^{12}$ cm^{-3}

experiments. The slopes given in the last columns are displayed in Fig. 3 as a function of partial pressure of O_2. For clarity, averages of the slopes are plotted for experiments with similar O_2 pressures. The curves in Fig. 3 represent results from computer modeling of the reaction system. These results will be discussed in the following section and it will be shown that the marked increase of the slope with pressure of O_2 is due to the very efficient reaction (1).

Table 1
Conditions and results of the experiments without O_2 present in the reaction system

P_{O_2} (lamp) mbar	P_{N_2} mbar	P_{H_2O} mbar	$[HO]_0$ 10^{12} cm^{-3}	initial slope, S_{II} 10^{-11} cm^3 s^{-1}
0.0	993	0.232	1.83	4.28
0.0	993	0.236	1.21	2.66
0.0	988	0.260	1.61	2.49
0.0	988	0.264	1.46	3.51
0.0	988	0.267	1.75	2.32
0.0	988	0.267	2.25	2.83
0.0	989	0.292	1.94	2.78
7.4	984	0.297	1.33	3.28
7.4	984	0.326	2.25	4.99
0.0	988	0.337	1.94	2.64
7.4	984	0.343	1.46	3.14
0.0	988	0.357	0.73	4.11
7.4	984	0.404	2.07	4.23
7.4	984	0.459	1.83	3.76
8.0	988	0.489	1.61	4.62
7.5	997	0.504	1.90	4.28
7.5	988	0.504	1.90	4.62
7.4	984	0.539	2.09	2.66
7.4	984	0.557	2.09	2.66
7.4	987	0.565	2.09	2.90
7.4	986	0.567	3.24	3.04
0.0	985	0.585	5.84	2.42
7.5	986	0.609	1.83	3.51
7.4	996	0.644	1.83	2.57
0.0	971	0.650	5.84	2.14
0.0	996	0.692	5.84	2.42
5.1	996	0.705	3.24	3.52
10.1	998	0.714	2.92	3.81
7.6	998	0.716	2.44	3.33*)
15.0	998	0.725	1.46	2.90
7.5	986	0.730	1.61	3.00
22.1	998	0.738	1.53	3.57
7.5	988	0.750	1.94	3.38
7.4	995	0.971	2.92	2.95
21.3	984	1.999	2.44	1.90
21.3	984	2.084	2.09	2.66
21.3	984	2.173	2.29	2.38

*) Decay curve displayed in Fig. 2.

Discussion

The discussion is based on the assumptions that equal amounts of HO and H are formed in the photolysis of H_2O, that the absolute concentration of HO can be determined precisely, and that the H atoms are stoichiometrically converted to HO_2 in the presence of O_2.

The other reactive species which can be formed in the $H_2O-O_2-N_2$-photolysis system are O atoms the concentration of which was kept small. When photolysing H_2O at short wavelengths ($145 > \lambda > 105$ nm), metastable $O(^1D)$ atoms are generated with low quantum efficiency (0.1) [31]. Below 145 nm, LiF windows have a transmission of less than 60%. Furthermore, the intensity of flash lamps decreases with shorter wavelengths. To further reduce the output of the lamp at short wavelengths, the flash light was filtered by O_2 present in the lamp. O_2 at pressures of up to 21 mbar was added to the gas flow through the flash lamp particularly to minimize the photolysis of O_2 in the photolysis system. Metastable $O(^1D)$ atoms which might be formed in the present system are rapidly quenched by the large amount of N_2 to give ground state $O(^3P)$. It has been recently shown that the presence of O atoms can retard the decay of HO [14, 17]. In the present system, the concentration of O atoms is estimated not to exceed a few percent of that of HO. As will be shown later by computer modeling, this concentration will barely effect the fate of HO radicals in the present system. Moreover, the experiments with different pressures of O_2 in the flash lamp (Table 1 and Table 2) do not give any indication of significant amounts of O atoms in the reaction system.

In order to estimate a value for the rate constant of reaction (1), k_1, the removal of HO from the present system will be discussed using the reaction scheme given in Table 3. It is well known that, in the absence of O_2, reactions (2) to (5) are the relevant steps. In the presence of O_2, reactions (1) to (6) are of major importance. In computer calculations which will be discussed later, also reactions (7) to (16) are included for completeness. Rate constants were taken from the latest evaluations of rate data [23, 25, 32] except the data for reactions (14) to (16) which are specific for the present system and were estimated according to our previous experience. Furthermore, the value for k_3 was taken to be $6 \cdot 10^{-12}$ cm^3 s^{-1} (N_2, at 987 mbar) [33], a factor of two lower than the only literature value [34]. The

Table 2
Conditions and results of the experiments with O_2 present in the reaction system

P_{O_2} (lamp) mbar	P_{N_2} mbar	P_{H_2O} mbar	P_{O_2} (reactor) mbar	$[HO]_0$ 10^{12} cm^{-3}	initial slope, S_{III} 10^{-11} cm^3 s^{-1}
21.3	984	0.351	0.039	2.09	13.9
21.3	984	0.351	0.039	1.12	14.9
21.3	984	0.819	0.039	2.09	11.2
21.3	984	1.557	0.039	2.92	9.5
21.3	984	2.717	0.037	4.81	10.1
7.5	998	0.640	0.052	1.17	12.9
7.5	988	0.933	0.049	1.83	13.4
7.5	988	0.945	0.049	1.83	13.0
7.5	994	0.984	0.051	1.83	13.0
7.5	994	1.002	0.051	1.94	13.1
7.4	995	0.250	0.063	1.62	14.4
7.4	995	0.315	0.063	1.62	10.7
21.3	984	0.372	0.067	1.04	15.6
7.4	996	0.392	0.063	3.65	14.5
7.4	995	0.499	0.065	3.65	15.9
21.3	984	0.527	0.065	1.21	9.9
7.4	994	0.593	0.063	4.86	14.0
7.4	985	0.656	0.053	5.84	11.4
7.4	991	0.673	0.064	3.24	12.3
21.3	984	0.825	0.067	2.25	13.5
7.4	992	1.009	0.063	3.24	15.6
21.3	984	1.097	0.065	2.09	14.5
21.3	984	1.572	0.065	2.66	12.7
21.3	984	2.095	0.064	5.84	14.3
21.4	984	2.213	0.057	4.86	11.0
7.5	993	0.592	0.101	1.75	16.6
7.5	988	0.615	0.097	1.46	10.5
7.5	993	0.619	0.101	2.09	15.5
7.5	993	0.619	0.101	1.75	12.3[a]
7.4	986	0.633	0.093	4.18	11.2
5.1	998	0.726	0.102	7.3	13.7
7.6	998	0.730	0.102	2.66	15.1
10.0	998	0.733	0.103	2.66	15.5
7.5	986	0.837	0.109	1.75	12.7
7.5	986	0.861	0.109	1.21	14.6
7.5	986	0.877	0.122	1.75	13.3
7.4	986	0.616	0.213	2.92	12.3
7.4	978	0.641	0.229	4.86	15.3
7.5	993	0.583	0.336	1.53	14.9
7.4	978	0.618	0.314	4.86	15.7
7.4	986	0.629	0.350	4.86	18.2
21.3	984	0.715	0.340	5.84	16.2
7.5	997	0.585	0.371	1.53	13.6
7.5	994	0.588	0.387	1.53	13.1
7.5	994	0.588	0.387	1.83	15.1
7.5	986	0.870	0.465	1.61	14.0
7.5	986	0.893	0.465	1.75	15.7
7.5	986	0.904	0.465	1.61	14.1

[a] Decay curve displayed in Fig. 2.

literature value for k_2 [30] was increased by 33% in accordance with Lii et al. [10] to result in a better fit in the absence of O_2.

An upper limit for k_1 can now be estimated easily assuming that secondary production of HO is negligeable and that the initial removal of HO in the presence of O_2 occurs solely in a second order process by reaction (1). For these assumptions, Fig. 3 gives $k_1 < 1.4 \cdot 10^{-10}$ cm^3 s^{-1} from the average of all slopes with O_2 present.

A more realistic estimate can be obtained considering reactions (1) to (6). In the absence of O_2, with the initial concentration $[HO]_0 = [H]_0$, one obtains

$$\frac{1}{[HO]_t} - \frac{1}{[HO]_{t=0}} = (2k_2[N_2] + 3k_4 + k_3[N_2])\,t = S_{II} \cdot t \quad \text{(II)}$$

Table 3
Reactions and rate constants used in the present work

No.	Reaction	Rate constant[a]	Reference
1	$HO + HO_2 \rightarrow H_2O + O_2$	$1.05 \cdot 10^{-10}$	this work
2	$HO + HO + N_2 \rightarrow H_2O_2 + N_2$	$8.0 \cdot 10^{-12}$	30, 10
3	$HO + H + N_2 \rightarrow H_2O + N_2$	$6.0 \cdot 10^{-12}$	33, 34
4	$HO + HO \rightarrow H_2O + O$	$1.8 \cdot 10^{-12}$	25
5	$HO + O \rightarrow O_2 + H$	$3.3 \cdot 10^{-11}$	25
6	$H + O_2 + N_2 \rightarrow HO_2 + N_2$	$1.4 \cdot 10^{-12}$	25
7	$HO + H_2O_2 \rightarrow H_2O + HO_2$	$1.7 \cdot 10^{-12}$	25
8	$HO_2 + O \rightarrow HO + O_2$	$4.0 \cdot 10^{-11}$	25
9	$HO_2 + H \rightarrow HO + HO$	$3.2 \cdot 10^{-11}$	23
10	$HO_2 + H \rightarrow H_2 + O_2$	$1.4 \cdot 10^{-11}$	23
11	$HO_2 + H \rightarrow H_2O + O$	$5 \cdot 10^{-13}$	23
12	$HO_2 + HO_2 \rightarrow H_2O_2 + O_2$	$2.5 \cdot 10^{-12}$	25
13	$H + H + N_2 \rightarrow H_2 + N_2$	$2.0 \cdot 10^{-13}$	32
14	$HO \rightarrow$ wall	8 s^{-1}	b)
15	$HO_2 \rightarrow$ wall	4 s^{-1}	b)
16	$H \rightarrow$ wall	32 s^{-1}	b)

[a] Rate constants at 985 mbar N_2 and 298 K in units cm^3 s^{-1} if not otherwise stated.
[b] Estimated for the present system.

for short reaction times, t. It is assumed in this equation that reaction (5) follows reaction (4) immediately. In the presence of sufficient amounts of O_2, H atoms are efficiently converted to HO_2, $[H]_{t>0} = O$. Hence, with $[HO]_0 = [HO_2]_0$ one obtains

$$\frac{1}{[HO]_t} - \frac{1}{[HO]_{t=0}} = (2k_2[N_2] + 3k_4 + k_1)\,t = S_{III} \cdot t\,. \quad \text{(III)}$$

S_{II} and S_{III} in Eqs. (II) and (III) correspond to the initial slopes of the respective decay curves of Fig. 2 (dashed lines). These slopes are also listed in Tables 1 and 2 and are shown in Fig. 3 as a function of added O_2. Thus the difference of the slopes

$$S_{III} - S_{II} = k_1 - k_3\,[N_2] \quad \text{(IV)}$$

and the value for $k_3[N_2]$ determine k_1 to be $1.1 \cdot 10^{-10}$ cm^3 s^{-1}. The value for $k_3[N_2]$ (Table 3) is relatively small and contributes to the given value of k_1 by less than 5%.

It is interesting to note that the result of this simplified treatment is independent of the choice of the values for k_2 and k_4 and, of course, of the initial radical concentration.

To support the present value of k_1, decays of HO were simulated by computer calculations using all reactions and rate constants of Table 3. Examples of such simulations are given in Fig. 2 by full lines. Similar calculated HO decays were generated for different O_2 pressures in the reaction system using the average of the initial concentration of HO of $2.55 \cdot 10^{12}$ cm^{-3}. The decays were processed like the experimental data, i.e. the initial slopes of plots like those shown in Fig. 2 were plotted as a function of pressure of O_2. The result of this procedure is displayed in Fig. 3 by the full line, A, showing good agreement with the experimental data when using $k_1 = 1.05 \cdot 10^{-10}$ cm^3 s^{-1}. The sensitivity of this treatment to the value of k_1 is demonstrated by the two dashed curves in Fig. 3, B and C. These curves were generated using $k_1 = 1.25 \cdot 10^{-10}$, B, and $k_1 = 0.85 \cdot 10^{-10}$ cm^3 s^{-1}, C. Clearly, both these fits are poorer than the fit represented by the full line.

In the experiments, the initial HO concentration, $[HO]_0$, was varied. Therefore, the simulation was repeated for high concentrations, $[HO]_0 = 6 \cdot 10^{12}$ cm^{-3}, and for low concentrations, $[HO]_0 = 1.1 \cdot 10^{12}$ cm^{-3}. Again, the calculated HO decays were

represented in second order plots such as Fig. 2. Within the error limits the calculations were found to agree with the experimental data. The initial slopes of these plots are represented in Fig. 3 by the dashed lines D and E. As expected for dominant second order processes the variation of $[HO]_0$ influences these slopes only slightly.

The presence of O atoms can influence the HO concentration by reactions (5) and (8). Therefore, different initial concentrations of O atoms, $[O]_0$, were introduced into the simulation. The HO decays were always found to be slower for $[O]_0 > 0$. For example, with $[O]_0 = 0.1 \times [HO]_0$, k_1 had to be increased by 5% to make compensation for the production of HO by O atoms. This concentration of $[O]_0$ is estimated to be a safe upper limit of photolytically generated atoms.

Additional errors can be caused by non-uniform radical concentrations in the reactor. To estimate these errors, the decay of HO was simulated using a simplified kinetic and spatial model. Namely, the HO radicals were assumed to react solely according to second order:

$$[HO]_t = ([HO]_{t=0}^{-1} + kt)^{-1} . \quad (V)$$

Here, k represents a second order rate constant such as S_{II} or S_{III} of Eqs. (II) or (III). Moreover, the depth of the reactor was divided into sixteen absorbing layers (16 transversals of the probing light beam). The length was divided into four equal boxes.

For the unrealistic assumption that only half of the reactor was illuminated and the other half not, this model results in a value of the rate constant k_1 which is half of that reported in this work. A complete failure of half of the electrodes, however, was never observed. To further confine the error limits a worst case for the distribution of the radical concentration was conservatively assumed, namely 1.8, 1.4, 0.6, and 0.2 times the average (measured) HO concentration in the respective boxes. Also, such a large inhomogeneity seems to be strongly exaggerated considering the observed intensity fluctuations of the single electrodes (±30%). The concentration gradient in the depth of the reactor was calculated using an average absorption coefficient of H_2O of 100 cm^{-1} atm^{-1}. The decay of HO thus simulated was graphically evaluated by the same procedure applied to the present experimental data (Fig. 2), i.e. second order rate constants were obtained from reaction times of up to 16 ms. This simulation requires a rate constant k_1 about 15% smaller than that calculated for an homogeneous radical concentration. Inspite of the large inhomogeneity considered, such a small error is not surprising. For, at long reaction times, Eq. (V) determines $[HO]_t$ mainly by kt and not by $[HO]_{t=0}$. With all the errors considered, we estimate the value of the rate constant k_1 to be accurate within +25%; −35%.

It should be noted that the value of k_1 obtained by the present detection method depends linearly on the oscillator strength used. We have chosen the value of $f_{00} = 7.05 \cdot 10^{-4}$ reported by Golden et al. [26] since it was derived under similar experimental conditions. It has been also used in several previous kinetic studies [29, 30, 34]. However, there are more recent determinations of Einstein coefficients for $HO(A^2\Sigma^+, v' = 0 \rightarrow X^2\Pi, v'' = 0)$ transitions [27, 35, 36] which result in values of oscillator strengths, $f_{J'',J'}$ being 46% larger than those used in the present study. Thus, a value of k_1 as high as $1.5 \cdot 10^{-10}$ cm^3 s^{-1} cannot be completely excluded until the method of detection has been further confirmed.

Table 4
Literature values of the rate constant, k_1, for the reaction HO + HO_2 at room temperature

k_1 / 10^{-11} cm^3 s^{-1}	T / K	P (added gas) / mbar	References
20 ± 3	298	1000 (Ar)	Hochanadel, Ghormley, and Ogren (1972) [3]
16	298	930 (N_2 + O_2)	DeMore and Tschuikow-Roux (1974) [4]
5.1 ± 1.6	293	a few mbar	Burrows, Harris, and Thrush (1977) [5]
3.0 ± 1.0	293	1.45–3.1 (He)	Hack, Preuss, and Wagner (1978) [6]
2–3	295	2.8–5 (He)	Chang and Kaufman (1978) [7]
5.1 ± 1.7	298	2.7 (Ar, He)	Burrows, Cliff, Harris, Thrush, and Wilkinson (1979) [8]
12–13	298	1000 (N_2 + O_2)	DeMore (1979) [9]
9.9 ± 1.2	308	1600 (Ar)	Lii, Gorse, Sauer, and Gordon (1980) [10]
11.7 ± 2.5	296	1000 (He)	Hochanadel, Sworski, and Ogren (1980) [11]
6.2 (+4; −2)	288–348	1000 (O_2 + N_2, He)	Burrows, Cox, and Derwent (1981) [12]
5.8 ± 0.9	298	2.7 (Ar)	Thrush and Wilkinson (1981) [13]
6.4 ± 1.5	299	1.33 (He)	Keyser (1981) [14]
7.5 ± 1.2	298	4 (He)	Sridharan, Qiu, and Kaufman (1981) [15]
9.9 ± 2.5	308	1000 (He, Ar or N_2)	Cox, Burrows, and Wallington (1981) [16]
6.7 ± 2.3	298	2–14 (He)	Temps and Wagner (1981) [17]
10–20	298	1000 (SF_6)	Kurylo, Klais, and Laufer (1981) [18]
11 (+2.8; −3.9)	298	985 (N_2)	this work
Reviews and Evaluations:			
2–20	300		Hampson and Garvin (1975) [19]
3	200–300		NASA (1977) [20]
3	200–300		Hampson and Garvin (1978) [21]
4	200–300		NASA (1979) [22]
3.5	298		Baulch et al. (1980) [23]
3.5	298		Hampson (1980) [24]
4	298		DeMore et al. (1981) [25]

In Table 4 the present value of k_1 is compared with values reported in the literature. It is interesting to note in this table that the values determined at about atmospheric pressure have decreased steadily from $2 \cdot 10^{-10}$ to about $1 \cdot 10^{-10}$ cm^3 s^{-1} and that, at low pressures, the values gradually increased from about $3 \cdot 10^{-11}$ to $7 \cdot 10^{-11}$ cm^3 s^{-1}. The present value is in very good agreement with the most recent values obtained at atmospheric pressure [9–11, 16, 18]. Within the estimated error limits, the present value also agrees with the largest value ($7.5 \cdot 10^{-11}$ cm^3 s^{-1}) [15] gained from discharge flow experiments. Moreover, the error limits of all recent determinations at low pressures [14, 17] with the exception of one [13] overlap with that of the present value. It therefore appears to be difficult with the current precision to decide whether the kinetics of reaction (1) depends on pressure or not. Also, no dependence on pressure of H_2O (0.25 to 2.7 mbar) was observed in the present work. Thus, it does not appear to be likely that H_2O plays a role as a complexing agent.

Preliminary experiments of this work have been supported by the Umweltbundesamt. The continuation of the experiments has been supported by a grant of the Deutsche Forschungsgemeinschaft. The authors thank Prof. Dr. H. Gg. Wagner for his suggestion to consider inhomogeneities of the radical concentrations and Priv. Doz. Dr. J. Warnatz for providing us with the computer program.

References

[1] H. W. Biermann, C. Zetzsch, and F. Stuhl, Ber. Bunsenges. Phys. Chem. *82*, 633 (1978).
[2] See for example: M. Nicolet, "Etude des réactions chimiques de l'ozone dans la stratosphère", Institute Royal Météorologique de Belgique, Brüssel, 1980.
[3] C. J. Hochanadel, J. A. Ghormley, and P. J. Ogren, J. Chem. Phys. *56*, 4426 (1972).
[4] W. B. DeMore and E. J. Tschuikow-Roux, J. Phys. Chem. *78*, 1447 (1974).
[5] J. P. Burrows, G. W. Harris, and B. A. Thrush, Nature *267*, 233 (1977).
[6] W. Hack, A. W. Preuss, and H. Gg. Wagner, Ber. Bunsenges. Phys. Chem. *82*, 1167 (1978).
[7] J. S. Chang and F. Kaufman, J. Phys. Chem. *82*, 1683 (1978).
[8] J. P. Burrows, D. I. Cliff, G. W. Harris, B. A. Thrush, and J. P. T. Wilkinson, Proc. R. Soc. London A *368*, 463 (1979).
[9] W. B. DeMore, J. Phys. Chem. *83*, 1113 (1979).
[10] R. R. Lii, R. A. Gorse, Jr., M. C. Sauer, Jr., and S. Gordon, J. Phys. Chem. *84*, 819 (1980).
[11] C. J. Hochanadel, T. J. Sworski, and P. J. Ogren, J. Phys. Chem. *84*, 3274 (1980).
[12] J. P. Burrows, R. A. Cox, and R. G. Derwent, J. Photochem. *16*, 147 (1981).
[13] B. A. Thrush and J. P. T. Wilkinson, Chem. Phys. Lett. *81*, 1 (1981).
[14] L. F. Keyser, J. Phys. Chem. *85*, 3667 (1981).
[15] U. C. Sridharan, L. X. Qiu, and F. Kaufman, J. Phys. Chem. *85*, 3361 (1981).
[16] R. A. Cox, J. P. Burrows, and T. J. Wallington, Chem. Phys. Lett. *84*, 217 (1981).
[17] F. Temps and H. Gg. Wagner, Ber. Bunsenges. Phys. Chem. *86*, 119 (1982).
[18] M. J. Kurylo, O. Klais, and A. H. Laufer, J. Phys. Chem. *85*, 3674 (1981).
[19] R. F. Hampson, Jr. and D. Garvin (Editors), Nat. Bur. Stand. (U.S.) Techn. Note 866 (1975).
[20] NASA Ref. Publ. 1010 "Chlorofluoromethanes and the Stratosphere", R. D. Hudson, Editor (1977).
[21] R. F. Hampson, Jr. and D. Garvin, Editors, Nat. Bur. Stand. (U.S.) Spec. Publ. 513 (1978).
[22] NASA RP 1049 "The Stratosphere: Present and Future", R. D. Hudson and E. I. Reed, Editors (1979).
[23] D. L. Baulch, R. A. Cox, R. F. Hampson, Jr., J. A. Kerr, J. Troe, and R. T. Watson, J. Phys. Chem. Ref. Data, *9*, 295 (1980).
[24] R. F. Hampson, Jr., "Chemical Kinetic and Photochemical Data Sheets for Atmospheric Reactions", Federal Aviation Administration, Report No. FAA-EE-80-17, U.S. Department of Transportation, 1980.
[25] W. B. DeMore, L. J. Stief, F. Kaufman, D. M. Golden, R. F. Hampson, M. J. Kurylo, J. J. Margitan, M. J. Molina, and R. T. Watson, "Chemical Kinetic and Photochemical Data for Use in Stratospheric Modelling, Evaluation Number 4: NASA Panel for Data Evaluation", JPL Publication 81-3, 1981, Jet Propulsion Laboratory, California Institute of Technology, Pasadena, California.
[26] D. M. Golden, F. P. Del Greco, and F. Kaufman, J. Chem. Phys. *39*, 3034 (1963).
[27] A. Goldman and J. R. Gillis, J. Quant. Spectrosc. Radiat. Transfer *25*, 111 (1981).
[28] G. Wagner and R. Zellner, Ber. Bunsenges. Phys. Chem. *85*, 1122 (1981).
[29] R. P. Overend, G. Paraskevopoulos, and R. J. Cvetanović, Can. J. Chem. *53*, 3374 (1975).
[30] D. W. Trainor and C. W. von Rosenberg, Jr., J. Chem. Phys. *61*, 1010 (1974).
[31] L. J. Stief, W. A. Payne, and R. B. Klemm, J. Chem. Phys. *62*, 4000 (1975).
[32] D. L. Baulch, D. D. Drysdale, D. G. Horne, and A. C. Lloyd, "Evaluated Kinetic Data for High Temperature Reactions, Vol. 1: Homogeneous Gas Phase Reactions of the H_2-O_2 System", Butterworths, London 1972.
[33] R. Zellner, private communication.
[34] R. Zellner, K. Erler, and D. Field, Symp. Combust. 16th, Combustion Institute, Pittsburgh, 1977, p. 939.
[35] W. L. Dimpfl and J. L. Kinsey, J. Quant. Spectrosc. Radiat. Transfer *21*, 223 (1979).
[36] J. L. Chidsey and D. R. Crosley, J. Quant. Spectrosc. Radiat. Transfer *23*, 187 (1980).
[37] W. B. DeMore, J. Phys. Chem. *86*, 121 (1982).

(Eingegangen am 24. Februar 1982) E 5146

Vibrational Energy Flow and Distribution in CF_3J and CF_3 after Infrared Multiphoton Excitation

Matthias Kauer and Carlo Kleinermanns

Max-Planck-Institut für Strömungsforschung, Göttingen

Energieübertragung / Photochemie / Reaktionskinetik

Time and wavelength-resolved infrared emission techniques are used to study the multiphoton excitation and dissociation of CF_3J. Fluorescence is detected from the ν_1-(sym. CF_3-stretch), ν_4-(asym. CF_3-stretch), and ν_2-(sym. CF_3-deform.)-vibrational modes of CF_3J and at laserenergies exceeding the dissociation threshold also from CF_3 radicals and excited iodine atoms $J^*(^2P_{1/2} \rightarrow {}^2P_{3/2})$. – The pumped ν_1-ladder of states (ν_1, $v \geq 1$) is populated collision-free as the fluorescence rise times show. Strikingly different, the $\nu_4(v = 1)$-mode is populated via collisions, while the higher ν_4-states are populated collision-free. The $\nu_4(v = 1)$-population rate is measured to be $(7.1 \pm 2) \cdot 10^{13}$ cm^3 mol^{-1} s^{-1}. – The ν_1- and ν_4-emissions show a red-shift of the band peak and band broadning with increasing laser energy according to higher quanta excitation. – To longer observation times the ν_1- and ν_4-bands shift blue again and narrow somewhat according to vibrational relaxation. However at higher laser energies both band peaks do not shift back to their fundamental frequencies, but only decrease in intensity to longer times. This is interpreted as relaxation of these modes by coupling to low frequency modes like the C-J-vibrations, which can be easier V-R, T deactivated. – At laser energies exceeding the dissociation threshold a new emission band is found at 1245 cm^{-1}, due to the C-F-stretch of the vibrationally excited CF_3-radical. The rise of the fluorescence signal consists of two parts arising from initially vibrationally hot CF_3^+ and initially cold CF_3, which is subsequently excited by collisions with a rate of $(1.7 \pm 0.5) \cdot 10^{13}$ cm^3 mol^{-1} s^{-1}. – Activation- and deactivation rates for various spectral features of the vibrationally excited CF_3J molecule and CF_3 radical are presented.

Ber. Bunsenges. Phys. Chem. *86*, 602–606 (1982) – © Verlag Chemie GmbH, D-6940 Weinheim, 1982.
0005-9021/82/0707-0602 $ 02.50/0